Journal of ELECTRONIC MATERIALS, Vol. 37, No. 5, 2008
DOI: 10.1007/s11664-007-0327-x

Imaging Surface Pits and Dislocations in 4H-SiC by Forescattered Electron Detection and Photoluminescence

Y.N. PICARD,[1,2] K.X. LIU,[1] R.E. STAHLBUSH,[1] and M.E. TWIGG[1]

1.—Electronics Science and Technology Division, Naval Research Laboratory, Washington, DC 20375, USA. 2.—e-mail: yoosuf.picard@nrl.navy.mil

Forescattered electron detection (FED) was utilized to image surface depressions resulting from threading screw and edge dislocations in 4H-SiC epitaxial layers. These surface depressions, or growth pits, exhibited two morphology types. Screw and edge dislocations could be imaged by photoluminescence and differentiated by their interactions with propagating partial dislocations (PDs). Correlations between FED and photoluminescence showed that sharp-apex pits 1 μm in size and strip-shaped pits 500 nm in size could be linked to individual screw and edge dislocations, respectively. Forescattered electron detection demonstrated sufficient sensitivity to image surface features previously resolvable only by atomic force microscopy. This new technique is nondestructive, noncontact, and capable of rapid, spatial mapping of growth pits resulting from threading screw and edge dislocations in SiC epitaxial layers.

Key words: 4H-SiC, forescattered electrons, growth pits, surface depressions, photoluminescence, dislocations, epitaxial layers

INTRODUCTION

Various crystallographic defects are known to hinder the performance of SiC electronic devices.[1] Many of these crystalline defects produce morphological features visible by atomic force microscopy (AFM) or optical microscopy and can be correlated to the degradation of various electrical properties.[2] Certain surface morphological defects are in fact found to have "device killing" behavior.[3,4] Such fatal surface defects are primarily associated with polytype inclusions or stacking faults and produce large enough morphological features to be readily observable by optical microscopy.[4,5]

It has been previously argued that screw dislocations can also influence device characteristics, such as inhomogeneities in Schottky barrier heights[6] or the reverse leakage and breakdown properties of p–n junctions in 4H-SiC.[7] Screw dislocations were discovered to produce sharp-apex pits at SiC surfaces by correlating AFM imaging of these features with synchrotron white-beam X-ray topography (SWBXT).[8,9] Recent experimental results indicate that these sharp-apex pits might influence Schottky barrier height inhomogeneities by causing localized electric field enhancement.[10] Also, recent nondestructive analysis by SWBXT has indicated that closed core screw dislocations influence microplasma breakdown in 4H-SiC.[11] Therefore, analysis of screw dislocations and morphological features linked to such defects are crucial for further advancement of SiC device engineering. However, surface morphological features tied to screw or edge dislocations have not been easily resolvable by optical microscopy[8] without utilizing destructive measures such as KOH etching.

Alternative, nondestructive methods for surface morphological and dislocation analysis could help to resolve many outstanding issues regarding how screw or edge dislocations could limit SiC device performance. A recently developed nondestructive method using polarized light microscopy (PLM) has been developed to investigate crystallographic defects in 4H-SiC.[12] The PLM technique utilizes strain-induced birefringence to produce contrast features indicative of stress fields caused by crystal defects.[13] Stress striation areas observed by PLM

(Received July 16, 2007; accepted October 12, 2007; published online October 30, 2007)

and linked to threading screw or edge dislocations were found to correspond to surfaces decorated with sharp-apex pits and stripe-shaped pits resolved by AFM.[12] These pits have been difficult to locate by optical microscopy[8,12] and have only been imaged directly by AFM.

In this work, we introduce forescattered electron detection (FED) conducted in a commercial scanning electron microscope (SEM) as a means to directly image shallow (<50 nm) pits. Topological contrast in an SEM can be enhanced by tilting the specimen surface at an oblique angle to the incident electron beam and detecting forescattered electrons.[14] In fact, such a configuration has previously demonstrated direct topological imaging of atomic steps.[15,16] Images recorded by FED of regions containing surface features were compared to corresponding photoluminescence (PL) images of the same areas. PL has been previously utilized to image screw and edge dislocations in both 4H-SiC[17,18] and 6H-SiC[19] with molten KOH etching used for confirmation. It should be noted, however, that PL alone was unable to differentiate between edge and screw dislocations in those studies.[17–19]

EXPERIMENT

The specimens in this study were epitaxial 4H-SiC layered films grown on n-type 4H-SiC substrates off-cut 8° from the (0001) basal plane in the [11$\bar{2}$0] direction. The layered film structure was composed of a 16 μm n^+ buffer layer (2×10^{18} cm^{-3}), 115 μm n^- drift layer (2×10^{14} cm^{-3}), 2 μm p^+ anode layer (8×10^{18} cm^{-3}). Samples were cut from the original wafer substrate by a diamond dicing saw and cleaned in methanol. PL was conducted by ultraviolet (UV) excitation using primarily 351.1 and 363.8 nm lines from a Coherent Innova 90-5 argon ion laser. Spectra were filtered using a 780 nm long-pass filter and collected to form images using a liquid-nitrogen-cooled charge-coupled device. Forescattered electron detection was performed in a dual-beam instrument with SEM and focused ion beam capabilities. Samples were mounted with the surface normal tilted 70° from the incident 20 kV electron beam. Electrons forescattered from the sample surface were collected by diode detectors mounted on a commercially available electron backscatter diffraction (EBSD) system. The experimental set-up for FED is shown in Fig. 1. Digitized electron micrographs were recorded and adjusted for the 70° tilt using computer software. The [11$\bar{2}$0] off-cut direction runs from left to right for all FED, SED, and PL images in this study.

RESULTS

PL images of individual dislocations shown as bright spots are presented in Fig. 2. The PL image

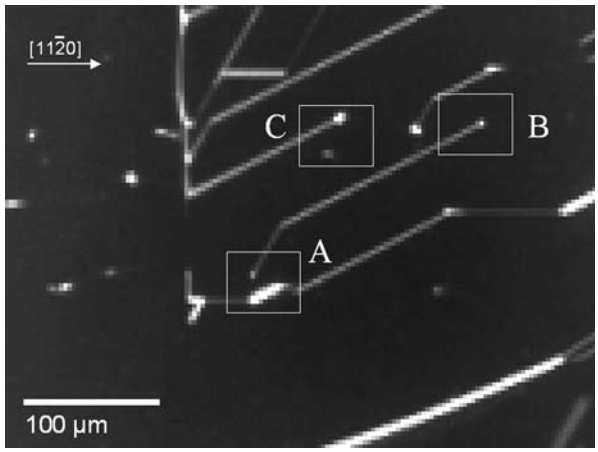

Fig. 2. PL image of dislocations (bright spots) that have interacted with partial dislocations to produce dislocation dipoles (bright line segments). Three areas were closely investigated by FED and are identified and labeled A to C. The arrow indicates the off-cut direction.

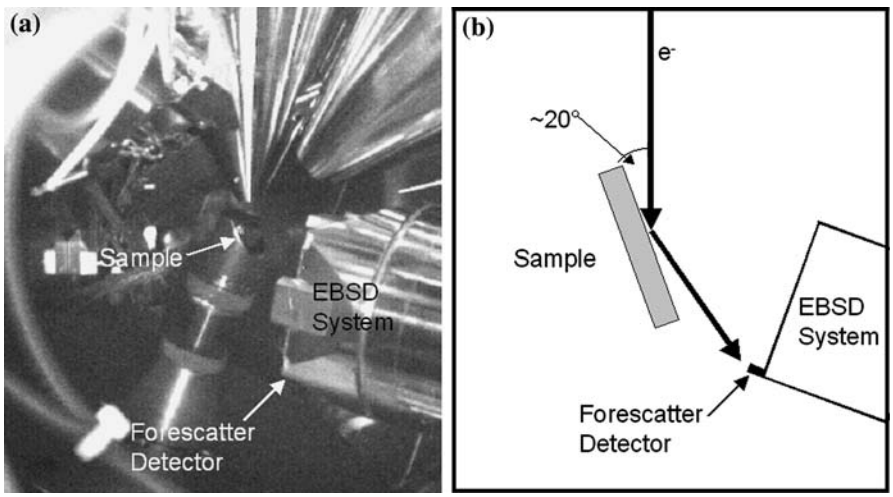

Fig. 1. Experimental set-up for FED imaging depicted (a) visually and (b) schematically.

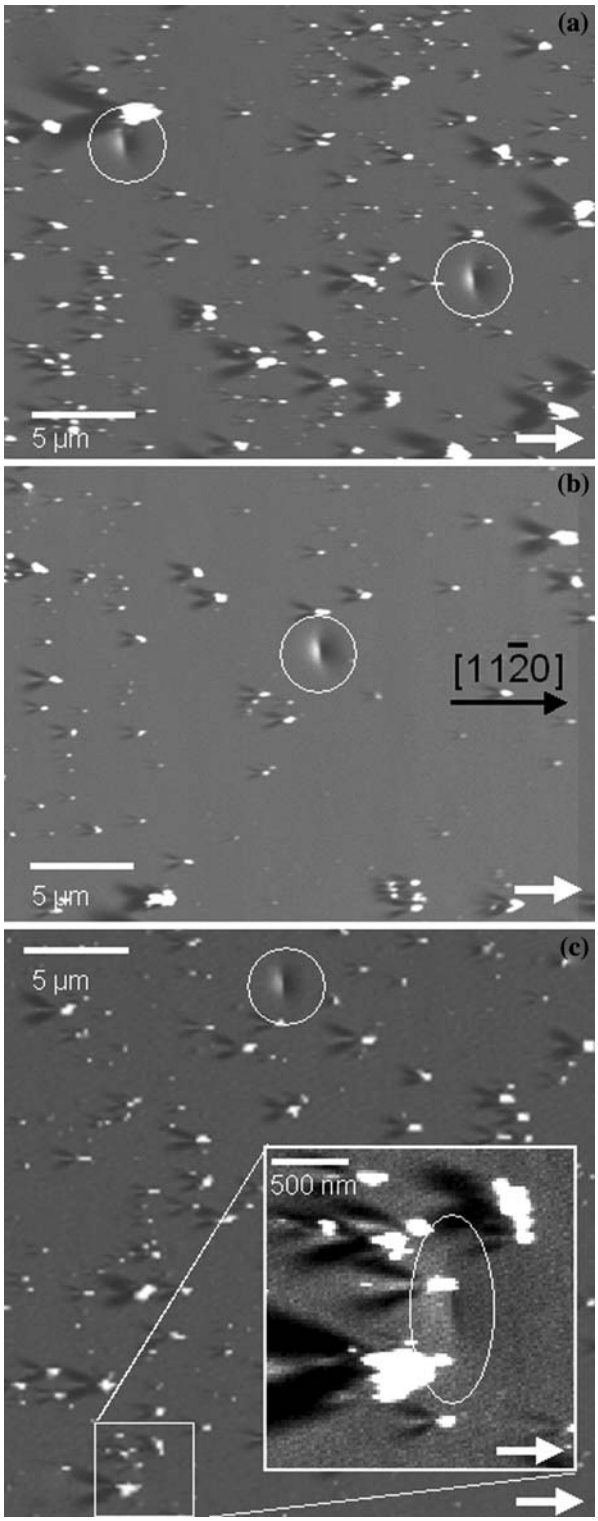

Fig. 3. FED micrographs of 4H-SiC surfaces corresponding to areas (a) A, (b) B, and (c) C in Fig. 2. Surface depressions (highlighted by circles) were found to correspond to screw dislocations imaged by PL in Fig. 2. A smaller, shallower pit (c) that corresponds to a suspected edge dislocation is shown in the inset.

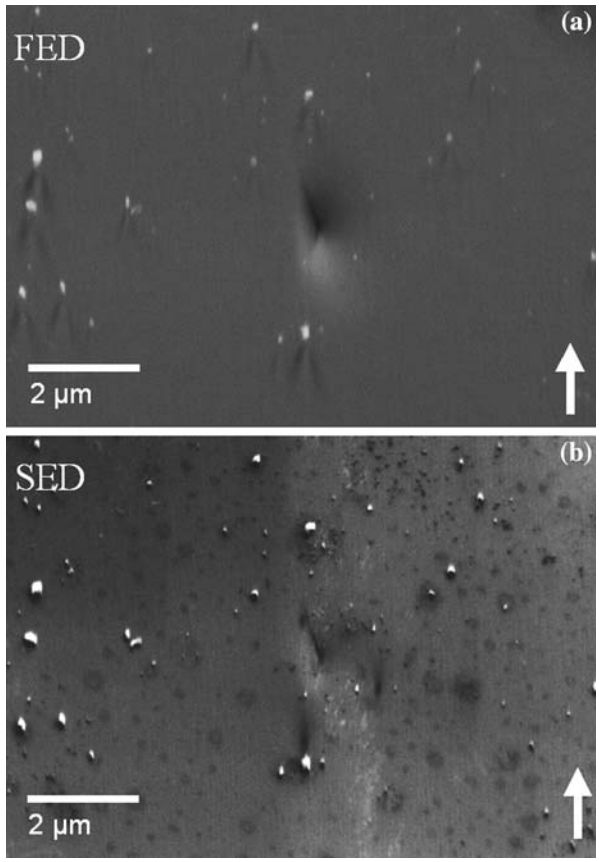

Fig. 4. Micrographs of a sharp-apex pit imaged by (a) FED and (b) conventional SED.

was recorded after Si-core partial dislocations (PDs) have passed through this region in the [$\bar{1}\bar{1}$20] direction (right to left). Three specific areas are highlighted in the figure and labeled A to C. Each of these areas encompasses at least one bright spot terminating at a bright line segment. Most of these bright spots are likely screw dislocations, while the bright line segments running along the $\langle 1\bar{1}00 \rangle$ directions are trailing PD dipoles. Propagating Shockley PDs have been shown to generate a trailing PD dipole upon intersecting a threading screw dislocation.[20] No such interaction has been evident between propagating PDs and threading edge dislocations. Since edge dislocations are luminescent under UV irradiation, they can be identified in Fig. 2 as specific bright spots not terminating at bright line segments. The rectangular area labeled C in Fig. 2 encompasses an isolated bright spot likely to be an edge dislocation. Propagation of PDs can be induced by any process that introduces electron–hole pairs,[21] such as the UV laser in the case of our study. These PL results provided an initial baseline for locating and distinguishing screw and edge dislocations with the assumption that at least one Shockley PD had propagated through every threading dislocation. This premise could not be used to distinguish screw and mixed dislocations since they are both likely to produce trailing PD dipoles upon interaction with a propagating PD.

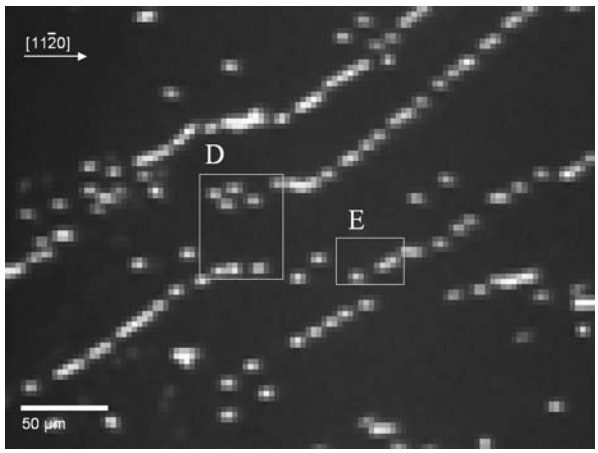

Fig. 5. PL image of suspected edge dislocations. Two areas were imaged at higher magnification by FED and are identified and labeled D and E.

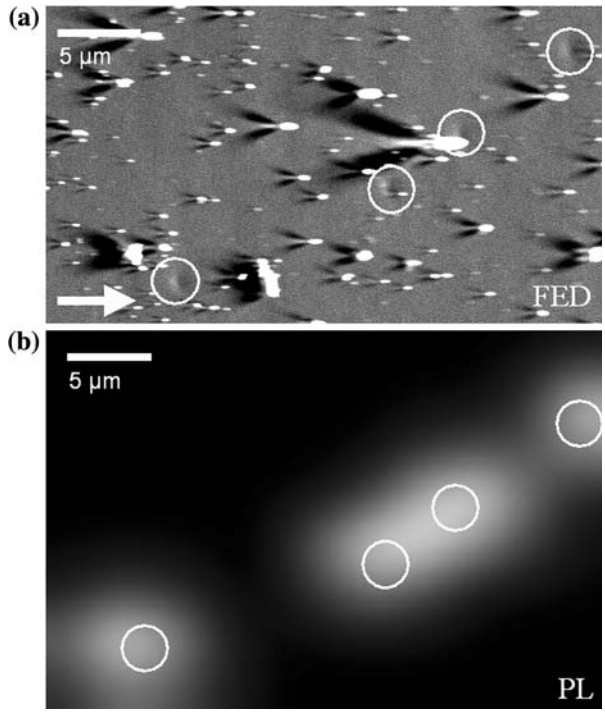

Fig. 7. Corresponding (a) FED and (b) PL images of the same 4H-SiC area labeled E in Fig. 5. White circles denote surface depressions found to correspond to edge dislocations identified by PL.

Figure 3 presents FED images of surfaces corresponding to the three areas highlighted by PL in Fig. 2. Significant debris resulting from the dicing process was present on the surface and utilized to compare artifacts to shallow surface depressions. White arrows in Fig. 3 denote both the direction of the incident electron beam and the relative position of the diode detectors used to record each image. The debris particles cast characteristic shadows opposite the relative direction of the two diode detectors. The resulting feature was a dark to bright (left to right) intensity variation that readily identifies particulates on top of the surface. Morphological features exhibited a different intensity variation and are denoted by white circles in Fig. 3. These features produce a more subtle but opposite dark to light intensity variation to the type attributed to surface particulates. These features are indicative of surface depressions, where a higher yield of forescattered electrons was detected near the left side of the depression and a lower yield was detected within the depression. The estimated size of these surface depressions are $\sim 1\ \mu$m in length along the [1$\bar{1}$00] direction.

The surface depressions observed in Fig. 3 were found to correspond exactly to the bright spots found by PL and shown in Fig. 2. Therefore, each screw dislocation identified by PL could be correlated to a characteristic surface depression.

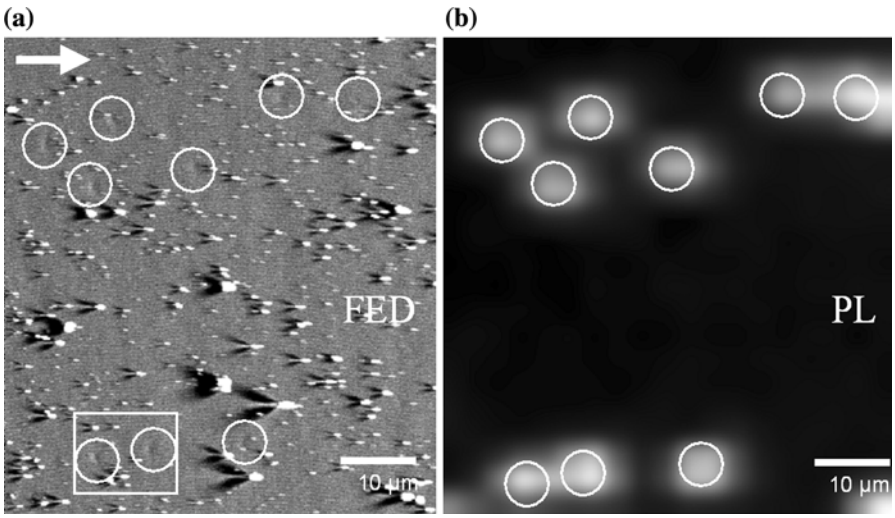

Fig. 6. Corresponding (a) FED and (b) PL images of the same 4H-SiC area labeled D in Fig. 5. White circles denote surface depressions found to correspond to edge dislocations identified by PL. The white rectangle highlights an area closely imaged by FED and SED shown in Fig. 8.

However, one of the dislocations identified by PL in area C of Fig. 2 was found to produce a much smaller and shallower depression. The small depression is shown in the inset of Fig. 3c. This small depression was roughly 500 nm in length along the [1$\bar{1}$00] direction. The stripe-shaped pit corresponded to a suspected edge dislocation based on the lack of observable interaction between PDs and this particular extended defect from PL (Fig. 2). A series of similar 500 nm long stripe-shaped pits have been previously observed by AFM corresponding to stress striations and dislocation walls heavily decorated with edge dislocations.[12] Imaging these surface depressions by AFM in that study required high-magnification scans over $\sim$10 μm $\times$ 10 μm areas. In our study, we observed similar surface depression using FED at similar magnifications but over larger areas.

A surface depression correlated to a threading screw dislocation was imaged in a different FED configuration and is presented in Fig. 4a. The relative position of the diode detectors are noted by white arrows in Fig. 4. With the diode detectors positioned 90° from the previous orientation, more features of the depression could be resolved. The sharp-apex noted in previous AFM studies[8,9] was discerned by FED and points towards the [11$\bar{2}$0] offcut direction. A comparative image of the same surface depression recorded by conventional secondary-electron detection (SED) is shown in Fig. 4b. Surface contamination was much more pronounced in the SED image and obscured the details of the surface depression. This observation highlights the advantages of using FED for topologically sensitive imaging of shallow surface depressions over SED, which is normally used in conventional SEM.

Figure 5 presents a PL image of an area of the SiC specimen characteristic of a high density of edge dislocations. The bright spots in the PL image were distributed into linear arrays, indicative of low-angle grain boundaries known to mostly be composed of edge dislocations.[17] Two specific areas are highlighted and labeled in Fig. 5 where PL and FED imaging are more closely compared. The comparative PL and FED images of the highlighted areas are presented in Figs. 6 and 7. Characteristic features indicative of shallow surface depressions were found to exactly correlate with the edge dislocations imaged by PL. These surface depressions were identical to the depression shown in the Fig. 3c inset, exhibiting the stripe-shaped morphology.

Particular surface depressions highlighted (rectangle) in Fig. 6 are presented in Fig. 8 at higher magnification. These surface depressions were imaged by conventional SED (Fig. 8a) and by FED in two orientations (Fig. 8b and c). The relative position of the diode detectors for each particular orientation is denoted by the white arrows in each FED image (Fig. 8b and c). The pits were elongated along the [1$\bar{1}$00] step edges and found to be completely invisible to conventional SED (Fig. 8a).

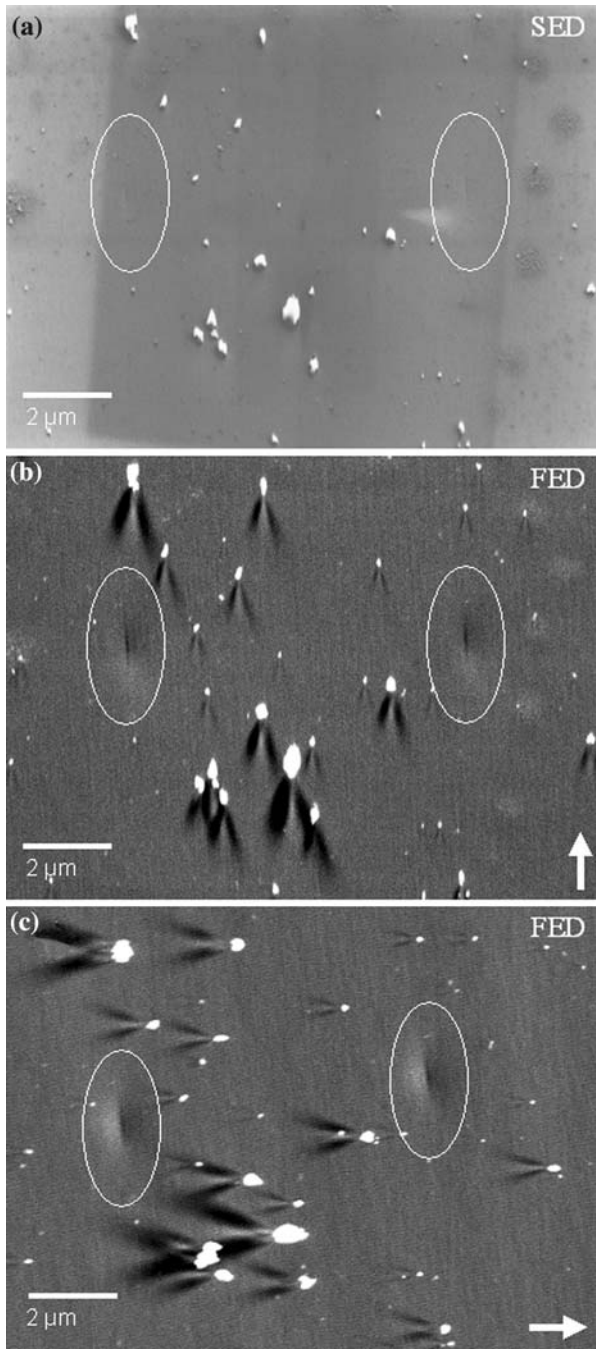

Fig. 8. (a) SED and (b, c) FED images of the area highlighted by the white rectangle in Fig. 6. White ellipses mark the location of shallow surface depressions found to correspond to edge dislocations identified by PL. White arrows indicate both the direction of the incident electron beam and the relative position of the diode detectors.

DISCUSSION

The larger surface depressions reported in this study have been previously referred to as growth pits. The formation of these growth pits is linked to partial impeding of step-flow homoepitaxial growth along basal plane surfaces by threading screw

dislocations.[8] The result is a sharp pointed depression with an apex and a small wake propagating in the downstep direction away from an individual threading dislocation. Such features have been difficult to observe at 1000 times magnifications by optical Nomarski microscopy.[12] According to Neudeck et al., these exceedingly small growth pits have not been accounted for in epiwafer manufacturing specifications.[8]

The size and shape of sharp-apex growth pits appear to be fairly consistent for various epilayer conditions. The depths of the sharp-apex pits have been reported as ~15 to 20 nm for 10 μm thick[8] or 3.5 μm thick epilayers.[9] The width of these sharp-apex pits along the step edges measured in both our study and others are typically about ~1 μm.[8,12] However, these growth pits have been shown to vary slightly in size for thicker epitaxial 4H-SiC layers.[12] Also, nanocores have been observed by AFM at the center of sharp-apex pits in designated high-quality epilayers and increase from 50 nm to 400 nm in size with greater epilayer thickness (from 10 μm to 100 μm in thickness). Nanocores inside the sharp-apex pits were not observed by FED in our study.

These surface depressions linked to threading screw and edge dislocations could have a significant impact on SiC devices. It is widely noted that surface characteristics are strongly connected to the overall performance of SiC Schottky-barrier-type devices.[6] Local field enhancement by sharp-apex pits is offered as an explanation for nonideal characteristics for Schottky barrier heights in SiC devices.[10] Field enhancement may also occur around the stripe-shaped pits linked to edge dislocations since they are of comparable size to sharp-apex pits and exhibit sharp features as well. However, direct imaging of these stripe-shaped pits has required high-magnification AFM.[12] Spatial mapping SiC surfaces by high-resolution AFM could prove arduous for detailing distributions of stripe-shaped pits. The FED technique has the advantage over AFM of being a noncontact technique, thus being capable of producing high-quality topological images of surfaces despite being contaminated by surface particulates. Hence, rapid and direct inspection of epitaxial SiC surfaces can be performed in a commercial SEM with the aim of determining growth pit densities and distributions.

The FED technique in our study has demonstrated the ability to directly image growth pits produced by threading screw and edge dislocations. Additionally, the FED approach can resolve the two different types of growth pits: sharp-apex pits (screw dislocations) and stripe-shaped pits (edge dislocations). The morphologies of sharp-apex and stripe-shaped growth pits were distinguishable at 3000 times magnification, as shown in Fig. 9. The morphologies were particular distinguishable by resolving the triangular shape of the sharp-apex pit when orienting the electron beam perpendicular to the off-cut direction (Fig. 9a and c). We found that stripe-shaped pits could be located at magnifications as low as 2000 times, while sharp-apex pits were resolvable down to 200 times. At present, the identification of mixed dislocations by morphological

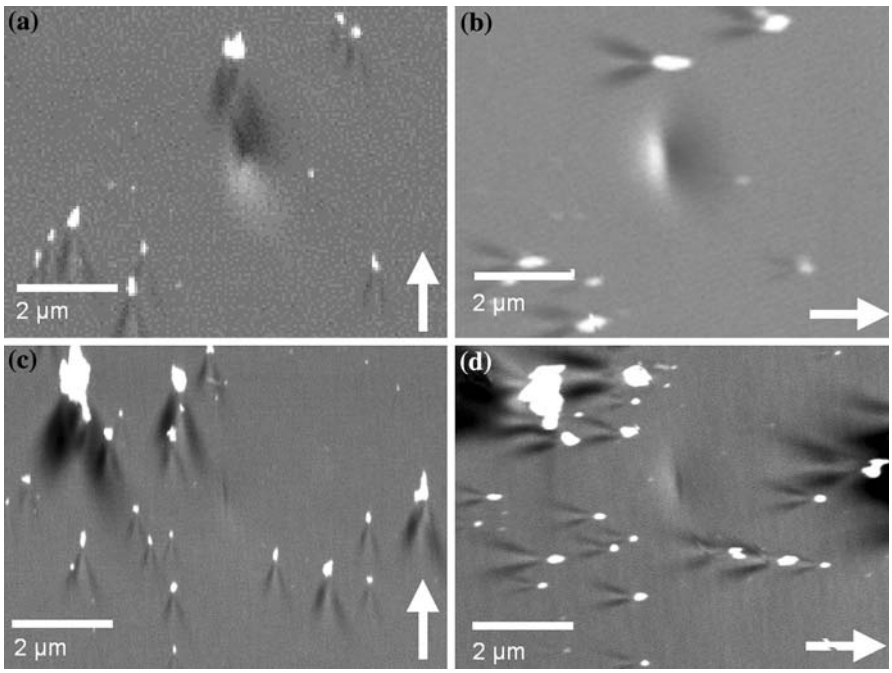

Fig. 9. FED images of (a, b) a sharp-apex growth pit and (c, d) a stripe-shaped growth pit. White arrows in the figure denote both the direction of the incident electron beam and the relative position of the diode detectors.

analysis of growth pits has not been explored. We note that the screw component of a mixed dislocation is likely to dominate growth pit formation. Hence, we suspect that both screw and mixed dislocations will produce quite similar growth pit morphologies, and distinguishing between them by FED may prove difficult.

CONCLUSIONS

The FED technique combined with PL imaging has been utilized to correlated surface depressions with screw or edge dislocations. Larger (1 μm sized) sharp-apex pits were directly correlated to threading screw dislocations. Other smaller stripe-shaped pits elongated (0.5 μm) along [$1\bar{1}00$] step edges were tied to threading edge dislocations. The FED technique demonstrates the ability to nondestructively image small pits previously resolvable only by AFM. The FED approach is thus found to be a powerful tool for noncontact nondestructive imaging of SiC epitaxial surfaces.

ACKNOWLEDGEMENTS

Work at the Naval Research Laboratory was supported by the Office of Naval Research. Two of the authors recognize financial assistance from the National Research Council (Y. Picard) and the American Society of Engineering Education (K. Liu).

REFERENCES

1. P.G. Neudeck, *Mater. Sci. Forum* 338–342, 1161 (2000).
2. Y. Wang, G.N. Ali, M.K. Mikhov, V. Vaidyanathan, B.J. Skromme, B. Raghothamachar, and M. Dudley, *J. Appl. Phys.* 97, 013540 (2005).
3. T. Kimoto, N. Miyamoto, and H. Matsunami, *IEEE Trans. Electron. Dev.* 46, 471 (1999).
4. Q. Wahab, A. Ellison, A. Henry, E. Janzén, C. Hallin, J. Di Persio, and R. Martinez, *Appl. Phys. Lett.* 76, 2725 (2000).
5. T. Okada, T. Kimoto, K. Yamai, H. Matsunami, and F. Inoko, *Mater. Sci. Forum* 457–460, 521 (2004).
6. M. Bhatnagar, J. Baliga, H.R. Kirk, and G.A. Rozgonyi, *IEEE Trans. Electron. Dev.* 43, 150 (1996).
7. P.G. Neudeck, W. Huang, and M. Dudley, *IEEE Trans. Electron. Dev.* 46, 478 (1999).
8. P.G. Neudeck, M.A. Kuczmarksi, M. Dudley, W.M. Vetter, H.B. Su, L.J. Keys, and A.J. Trunek, *Mater. Sci. Res. Symp. Proc.* 622, T121 (2000).
9. C.M. Schnabel, M. Tabib-Azar, P.G. Neudeck, S.G. Bailey, H.B. Su, M. Dudley, and R.P. Raffaelle, *Mater. Sci. Forum.* 338–342, 489 (2000).
10. X. Ma, P. Sadagopan, and T.S. Sudarshan, *Phys. Stat. Sol.* 203, 643 (2006).
11. U. Zimmermann, J. Osterman, D. Kuylenstierna, A. Konstantinov, W.M. Vetter, and M. Dudley, *J. Appl. Phys.* 93, 611 (2003).
12. X. Ma, H. Chang, Q. Zhang, and T. Sudarshan, *J. Cryst. Growth.* 279, 425 (2005).
13. X. Ma, M. Parker, and T.S. Sudarshan, *Appl. Phys. Lett.* 80, 3298 (2002).
14. O.C. Wells, *Appl. Phys. Lett.* 16, 151 (1970).
15. C. Trager-Cowan, E. Sweeney, P.W. Trimby, A.P. Day, A. Gholinia, N.-H. Schmidt, P.J. Parbrook, A.J. Wilkinson, and I.M. Watson, *Phys. Rev. B.* 75, 085301 (2007).
16. Y.N. Picard, M.E. Twigg, J.D. Caldwell, C.R. Eddy Jr., P.G. Neudeck, A.J. Trunek, and J.A. Powell, *Appl. Phys. Lett.* 90, 234101 (2007).
17. A. Galeckas, J. Linnros, and P. Pirouz, *Mater. Sci. Forum* 433–437, 933 (2003).
18. R.E. Stahlbush, K.X. Liu, Q. Zhang, and J.J. Sumakeris, *Mater. Sci. Forum* 556–557, 295 (2007).
19. M. Tajima, E. Higashi, T. Hayashi, H. Kinoshita, and H. Shiomi, *Appl. Phys. Lett.* 86, 061914 (2005).
20. Y. Chen, M. Dudley, K.X. Liu, and R.E. Stahlbush, *Appl. Phys. Lett.* 90, 171930 (2007).
21. A. Galeckas, J. Linnros, and P. Pirouz, *Appl. Phys. Lett.* 81, 883 (2002).